ELSEVIER

Journal of Crystal Growth 241 (2002) 283–288

JOURNAL OF CRYSTAL GROWTH

www.elsevier.com/locate/jcrysgro

Compositional and structural analysis of Nd-doped GaSb bulk crystals grown by the vertical Bridgman technique

J.L. Plaza[a,*], P. Hidalgo[b], B. Méndez[b], J. Piqueras[b], E. Diéguez[a]

[a] *Departamento de Física de Materiales, Universidad Autónoma de Madrid, Cantoblanco 28049, Spain*
[b] *Departamento de Física de Materiales, Universidad Complutense, Madrid 28040, Spain*

Received 25 October 2001; accepted 9 March 2002
Communicated by J.B. Mullin

Abstract

Nd-doped GaSb bulk crystals with three different dopant concentrations have been grown by the vertical Bridgman technique. The axial segregation has been characterised by obtaining the effective segregation coefficient. Differences in the value of this coefficient show its dopant concentration dependence. Resistivity, carrier density and mobility have also been obtained showing the p-type nature of this material. Structural and compositional properties have been studied revealing some inclusions with high Nd concentration in the highest Nd-doped ingot. © 2002 Published by Elsevier Science B.V.

PACS: 81.05.Ea; 82.80.Ch

Keywords: A2. Gradient freeze technique; B2. Semiconducting III–V materials

1. Introduction

Rare earth (RE) doped semiconductors are very interesting materials due to their applications in optoelectronics. These systems show a temperature stable luminescent wavelength which is nearly independent of the semiconductor host. The interest in RE doped semiconductors is based on the future fabrication of new electroluminescent devices, which can combine both the luminescence of rare earth ions and the electronic properties of semiconductors [1,2].

When RE elements are introduced as trivalent ions in solids, they exhibit atomic-like optical transitions due to the incomplete 4f shell, which is shielded by the outermost filled $5s^2$ and $5p^6$ orbitals. These intra-4f transitions are parity forbidden in the free ion but are allowed when the RE ions are embedded in solids, due to the mixing of opposite parity states which is induced by the local electric fields in the solid host [3,4]. In this way the RE ions interact weakly with the host matrix and the wavelength of the intra-4f shell emission is only very slightly dependent on the host material and the environmental temperature.

It is well known that crystalline Si is the primary material for the fabrication of electronic devices. On the other hand and due to the fact that it is an

*Corresponding author. Tel.: +34-91-397-4784; fax: +34-91-397-8579.
E-mail address: jl.plaza@uam.es (J.L. Plaza).

0022-0248/02/$ - see front matter
PII: S0022-0248(02)01249-6

indirect band gap semiconductor, the efficient light emission is difficult to achieve [5,6]. As a consequence, direct band gap III–V compound semiconductor materials have been successfully used in the fabrication of optoelectronic devices [7]. RE ions have been incorporated into III–V semiconductors by doping during the growth process [8–10] or by ion implantation [11–15].

Among the different RE ions Nd has shown to be a good choice for controlling the surface charge at the semiconductor-dielectric interface [16].

In this work, the Nd distribution in Bridgman-grown GaSb ingots has been studied by means of atomic absorption spectrometry (AAS). Some electrical properties like carrier density, mobility, resistivity and conductivity type have also been investigated by means of van der Pauw Technique. Structural and compositional properties have been obtained by scanning electron microscope (SEM), energy dispersive X-ray analysis (EDAX) and Cathodoluminescence (CL).

2. Experiment

Nd-doped GaSb ingots were grown by the vertical Bridgman technique. High purity 99.9999% Ga and Sb and 99.9% Nd metal were used as starting materials. High quality quartz ampoules were used as crucibles and sealed in vacuum at 10^{-6} Torr. The ampoules were previously graphited by acetone pyrolysis at 1000°C in order to prevent the material sticking to the walls. The growth was carried out at a rate of 3 mm/h in a single-zone Bridgman furnace having a parabolic thermal profile being almost flat at the centre and presenting a linear gradient of 57°C/cm in the solidification region. An oscillation system enables the homogenisation of the melt before the growth process. The homogenisation time employed was 24 h. More details about the growth process can be found elsewhere [17].

Three different GaSb ingots were grown with initial Nd concentrations in the melt of $0.6\times10^{19}\,cm^{-3}$ (ingot (A)), $2.4\times10^{19}\,cm^{-3}$ (ingot (B)) and $2.2\times10^{20}\,cm^{-3}$ (ingot (C)). All of them were 60 mm long and 12 mm in diameter. Several wafers extracted from different positions along the ingot were cut perpendicular to the growth direction. Mechanical polishing with 5 and 1 μm alumina powder and chemical etching for 5 min with a CP4 type solution (1 CH_3COOH : 5 HF : 9 HNO_3 : 10H_2O) were carried out on these samples.

In order to study the Nd concentration along the ingots, AAS analysis was carried out by taking a small quantity of material (about 100 mg) from different wafers. This procedure enables us to study the axial Nd concentration in different zones of the ingots. A Perkin-Elmer 3110 spectrometer equipped with a Nd hollow cathode lamp was used. High quality Perkin Elmer Nd 1000 ppm standards were used for the calibration of the system. For the preparation of the solutions for AAS analysis, the material was first dissolved in acids ($5\,cm^3$ HCl + $1\,cm^3$ HNO_3) and slightly heated at 70°C about 15 min until the presence of solid particles was no longer observed. The volume of the samples was increased to $20\,cm^{-3}$ with a solution of H_2O–HCl 0.6 N. Only the ingots (B) and (C) were analysed because of the low concentration of Nd present in the ingot (A), which could not be detected due to the precision of our apparatus.

For the measurement of the electrical properties like resistivity, mobility and carrier density the van der Pauw technique at room temperature was used with magnetic fields perpendicular to the samples up to 7 kG. Indium dots were used as ohmic contacts, which were previously verified.

SEM images and EDAX analyses were carried out by using a Philips model XL30 coupled with an EDAX analyser model DX4i. The accelerating voltages were 25 kV. The CL data were obtained with a Hitachi S-2500 SEM at 77 K and 25 kV of accelerating voltages.

3. Results and discussion

In order to obtain the Nd concentration profiles along the ingots, AAS analyses were carried out in the highest doped ingots named as B and C. These profiles versus the solidified fraction are shown in Fig. 1 where the anomalous high concentration in the final stages of the growth due to the final transient state [18] have been removed. The

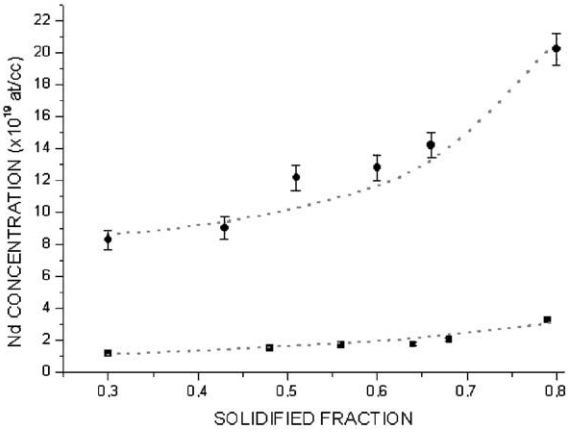

Fig. 1. Nd concentration profiles along the ingots (B) and (C) at the centre (●) and the periphery (■) of the wafers.

experimental points shown in Fig. 1 have been obtained as a mean value of the concentrations measured at the centre and at the periphery of the samples. These points can be fitted to the Scheil law, which relates the dopant concentration in the solid C_s with the initial concentration C_0 in the melt and the effective segregation coefficient K_{eff}.

In the case where the density in the solid, ρ^{sol} and in the liquid, ρ^{liq} have the same value, the Scheil law is given by the following expression:

$$C_s = K_{eff} C_0 (1-g)^{K_{eff}-1}, \quad (1)$$

where g is the solidified fraction. The mathematical development of this expression can be easily followed in Ref. [18]. On the other hand it must be pointed out that in the case of GaSb, the variation between ρ^{sol} and ρ^{liq} is nearly 8% ($\rho^{sol} = 5.6\,g\,cm^{-3}$ and $\rho^{liq} = 6.06\,g\,cm^{-3}$ [19]). This feature cannot be neglected and some corrections may be introduced in Eq. (1). This can be easily done by following the mathematical procedure for Eq. (1) given in Ref. [18]. In this way it is easy to show that when considering different values for ρ^{sol} and ρ^{liq}, the Scheil law is given by

$$C_s = K_{eff} C_0 (1-g)^{[(\rho^{sol}/\rho^{liq})K_{eff}-1]} \quad (2)$$

i.e. a correction term ρ^{sol}/ρ^{liq} to the value of the exponential K_{eff} appears. In the case of GaSb this correction term has a value of 0.924.

The results obtained for K_{eff} from the fit of the experimental points to the Eq. (2) are given in Table 1. The difference between the two values corresponding to the ingot (B) and (C) indicates the dependence of K_{eff} on the dopant concentration.

Table 1
Experimental values of the effective segregation coefficient, K_{eff} for the ingots (a) (B) and (b) (C) obtained from the Scheil law fit

Ingot	K_{eff}
(B)	0.14 ± 0.03
(C)	0.35 ± 0.04

Table 2
Resistivity, mobility and hole density obtained from van der Pauw technique for pure and Nd-doped GaSb

Ingot	Resistivity (Ω cm)	Mobility ($cm^2/V \cdot seg$)	Hole density ($\times 10^{17}\,cm^{-3}$)
Pure	0.0900	550	1.0
(A)	0.0854	410	1.8
(B)	0.0714	370	2.4
(C)	0.0273	230	10.0

Table 2 shows the resistivity, carrier mobility and density obtained by the van der Pauw technique on samples removed from the central region of the three ingots. All these samples showed p-type behaviour as has been previously reported for Er-doped GaSb [20]. It is worth noting that the increasing dopant concentration induces an increasing carrier density lowering the resistivity and mobility.

Some structural features of these materials have also been studied. Samples taken from different regions along the ingots were analysed by SEM. Fig. 2 shows several etch-pits revealed by chemical etching on a wafer extracted from ingot (A). The etch-pit density was about $5 \times 10^5\,cm^{-2}$. The quantitative data for the Ga and Sb concentrations inside and outside of the etch-pits, which are shown in Table 3 were obtained by EDAX analysis. It is observed that there is an excess of Ga inside the etch-pits. The presence of Nd could not be observed in the ingot (A) due to the poor sensitivity of EDAX at low dopant concentrations.

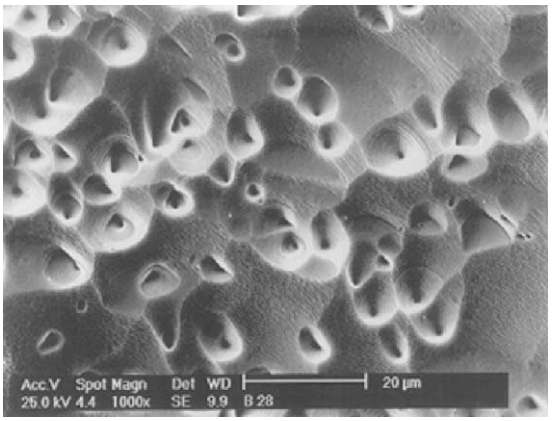

Fig. 2. Etch-pits at the surface of a wafer extracted from the central region of the ingot (A). Higher Ga concentrations inside the pits has been revealed by EDAX analysis.

Table 3
Concentration of Ga and Sb inside and outside the etch-pits shown in Fig. 2

Element	Concentration (at%) outside	Concentration (at%) inside
Sb	46.52	37.23
Ga	53.48	62.77

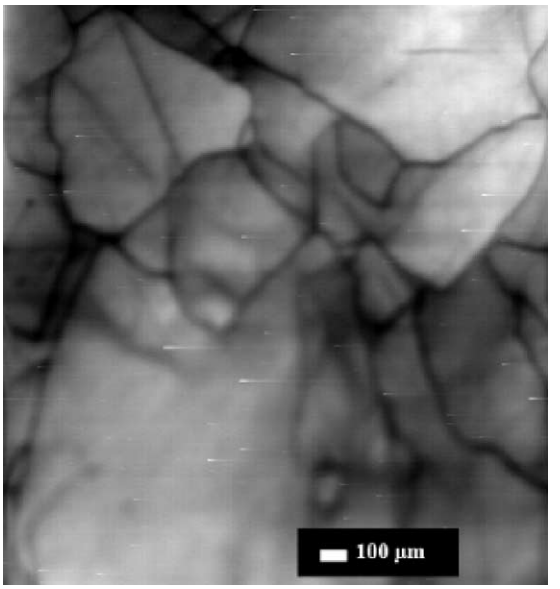

Fig. 3. CL image obtained from the sample (A) with the lowest initial dopant concentration.

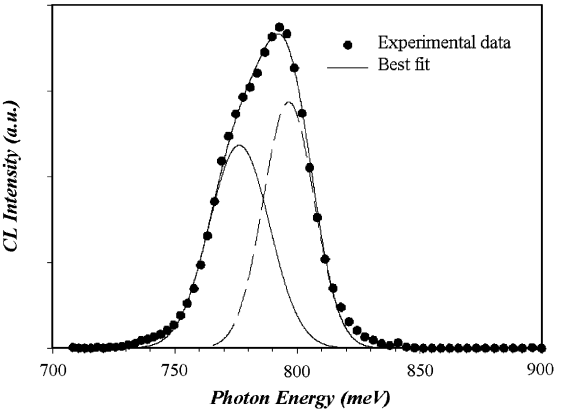

Fig. 4. CL spectrum from the sample (B). The continuous lines are the deconvoluted Gaussian bands that best fit the experimental points.

Cathodoluminescence (CL) images and spectra from the three ingots have been used to characterise the defect structure as a function of the Nd concentration. The samples for CL observations have been obtained from the central part of each ingot. In Fig. 3, a CL image from sample (A) is shown which reveals uniform bright background with dark lines that correspond to grain subboundaries [21] similar to that observed in undoped material. The CL spectrum, not shown for brevity, showed the near band edge emission and the native defects related band located at 777 meV usually observed in this material [21].

Regarding sample (B) with a higher Nd concentration, the SEM/EDAX analysis has revealed no main differences compared with the results obtained from sample (A). On the other hand, the increment in the dopant concentration shows a more inhomogeneous background in the CL images. In the CL spectrum corresponding to sample B and shown in Fig. 4 the defect band is detected and its intensity is comparable to the band gap emission.

In the sample (C) with the highest Nd concentration, it is important to note that some elongated inclusions with specific orientations and different sizes were observed at the final stages of the

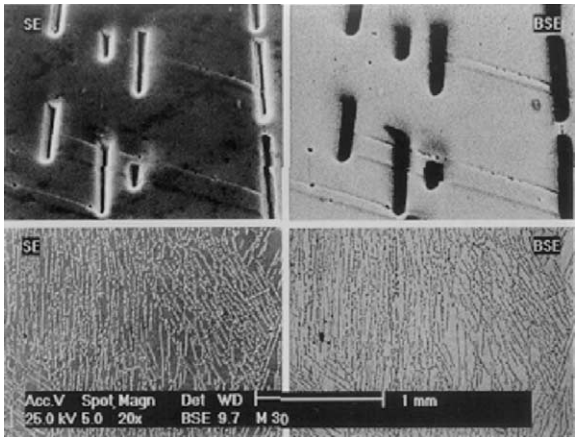

Fig. 5. Inclusions present at the final stages of the growth of the ingot (C).

Table 4
Concentration of Sb, Ga and Nd obtained inside and outside the inclusions observed in Fig. 3

Element	Concentration (at%) outside	Concentration (at%) inside
Sb	47.93	44.47
Ga	51.20	52.04
Nd	0.87	3.49

growth as shown in Fig. 5. In this figure both secondary electron (SE) and backscattering electron (BS) images are presented. The backscattering images give an idea of the compositional differences between the inclusions and the remaining surface in the samples. The EDAX analysis carried out inside and outside of the inclusions have shown that there is a higher concentration of Nd inside the inclusions which is about four times larger than outside. These etch-pits occur at some kind of Nd precipitation, which is removed during the chemical etching process. The Nd concentration data obtained by EDAX are shown in Table 4. It can be noted that some inclusions have also been observed in Er-doped GaSb crystals formed basically by Er and Sb [20].

The elongated inclusions could also be observed by CL as shown in Fig. 6A. It can also be observed from the CL spectrum shown in Fig. 6B that a remarkable decrease in the 777 meV band occurs. This effect of reduction of native defects has been

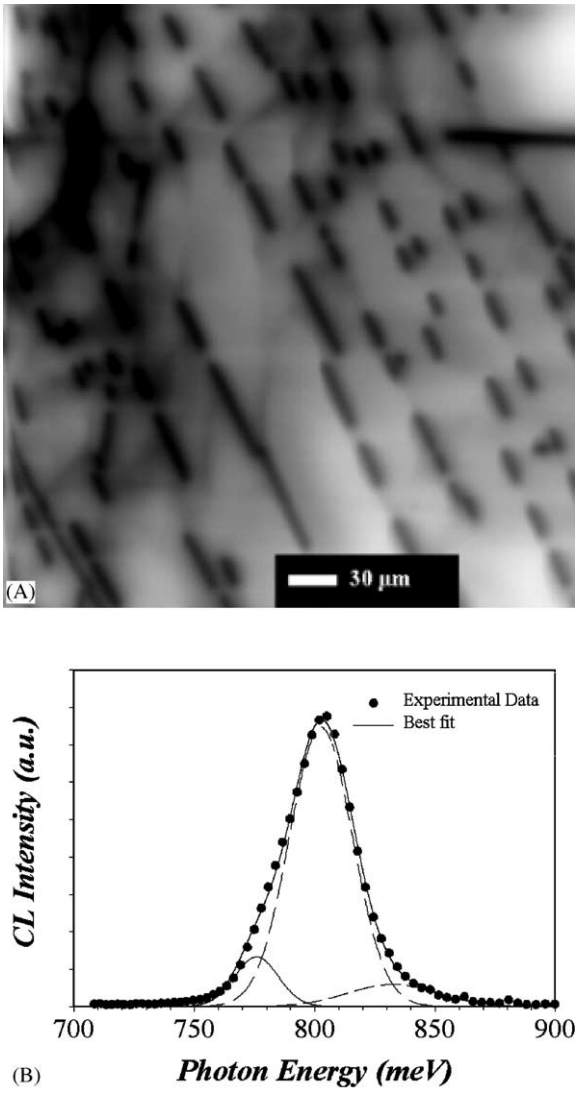

Fig. 6. CL (A) image and (B) spectrum from the sample (C). The continuous lines are the deconvoluted Gaussian bands that best fit the experimental points.

previously reported by doping with transition metals [22] and also with Er [23]. In the case of Nd, in addition to the reduction of the native defects, an enhancement of the luminescence intensity compared to other doped GaSb ingots obtained from Bridgman method is detected. A comparison with the EDAX results shows that the Nd effect of decreasing the defect band and

increasing the band gap intensity is limited by precipitation processes at high Nd concentrations.

4. Conclusions

In this work the segregation of Nd in Bridgman-grown GaSb ingots has been studied. The effective segregation coefficient has been obtained from the fit of the experimental dopant concentration data from AAS analysis to the Scheil Law. The results show that the values of these coefficients depend on the dopant concentration in the melt. The p-type behaviour and the decreasing resistivity with the increasing initial dopant concentration has been demonstrated by means of van der Pauw technique. SEM and CL analysis revealed the presence of inclusions with a high Nd concentration.

Acknowledgements

This work has been supported by CICYT under the project ESP-98 1340 and by INTAS-ESA Project number 99 01814.

References

[1] G.S. Pomrenke, P.B. Klein, D.W. Langer (Eds.), Rare Earth Doped Semiconductors, MRS Symp. Proc. No. 301, Materials Research Society, Pittsburg, 1993.
[2] S. Coffa, A. Polman, R.N. Schwartz, Rare Earth Doped Semiconductors II, MRS Symp. Proc. No. 422, Materials Research Society, Pittsburg, 1996.
[3] G.H. Dieke, Spectra and Energy Levels of Rare Earth Ions in Crystals, Wiley, New York, 1968.
[4] A.R. Zanatta, L.A.O. Nunes, Appl. Phys. Lett. 71 (25) (1997) 3679.
[5] S.M. Sze, Physics of Semiconductor Devices, Wiley, New York, 1981.
[6] L.T. Canham, Appl. Phys. Lett. 57 (1990) 1046.
[7] P. Bhattacharya, Semiconductor Optoelectronic Devices, Prentice-Hall, Englewood Cliffs, NJ, 1994.
[8] L.F. Zakharenkov, V.A. Kasatkin, F.P. Kesamanly, B.E. Samorukov, M.A. Sokolova, Sov. Phys. Semicond. 15 (1981) 946.
[9] V.A. Kasatkin, F.P. Kesamanly, V.G. Makarenkov, V.F. Masterov, B.E. Samorukov, Sov. Phys. Semicond. 14 (1980) 1092.
[10] V.A. Kasatkin, F.P. Kesamanly, B.E. Samorukov, Sov. Phys. Semicond. 15 (1981) 352.
[11] V.V. Ushakov, A.A. Gippius, V.A. Dravin, A.V. Spitsyn, Sov. Phys. Semicond. 16 (1982) 723.
[12] H. Ennen, U. Kaufmann, G. Pomrenke, J. Schneider, J. Windscheif, A. Axmann, J. Crystal Growth 64 (1983) 165.
[13] H. Ennen, J. Schneider, G. Pomrenke, A. Axmann, Appl. Phys. Lett. 43 (1983) 943.
[14] H. Ennen, G. Pomrenke, A. Axmann, J. Appl. Phys. 57 (1985) 2182.
[15] H. Ennen, J. Schneider, J. Electron Mater. 14A (1985) 115.
[16] T.J. Zhang, S.Y. Li, Solid State Electron. 29 (1986) 775.
[17] P.S. Dutta, H.L. Bhat, K.S. Sangunni, V. Kumar, in: A. Selvarajan, B.S. Sonde, K. Shenai, V.K. Tripathi (Eds.), Emerging Optoelectronic Technologies, Tata McGraw-Hill, New Delhi, 1992, 1991, p. 287;
P.S. Dutta, Thesis, Department of Physics, Indian Institute of Science, Bangalore, India, 1995.
[18] D.T.J. Hurle, Handbook of Crystal Growth, Vol. 2b, North-Holland, Amsterdam, 1994 (Chapter 12).
[19] P. Boiton, Thesis, Universite Montpellier II, 1996 p. 221.
[20] J.L. Plaza, P. Hidalgo, B. Méndez, J. Piqueras, J.L. Castaño, E. Diéguez, J. Crystal Growth 198–199 (1999) 379.
[21] B. Méndez, J. Piqueras, P.S. Dutta, E. Dieguez, Appl. Phys. Lett. 67 (1995) 2648.
[22] P. Hidalgo, B. Méndez, P.S. Dutta, J. Piqueras, E. Dieguez, Phys. Rev. B57 (1998) 6479.
[23] P. Hidalgo, B. Méndez, J. Piqueras, J. Plaza, E. Diéguez, Semicond. Sci. Technol. 13 (1998) 1431.